

Copper(II) Salen based Complexes as Potential Anticancer Agents

Nithya Mohan^a, Vidhya C.V.^b, Suni V.^b Jimna Mohamed Ameer^c, Naresh Kasoju^c, P. V. Mohanan^a,
Sreejith S. S. S.^d, *,^a and M. R. Prathapachandra Kurup *^{a, e}

Infrared Spectral Data

Infrared spectra of the four compounds are shown in Figure 1. The compound **1** shows a twin peak around 3500 cm^{-1} which indicate the presence of encapsulated water molecule and falls under the category of inclusion compounds.

Table S1 IR spectral values in cm^{-1} of compounds **1** to **4**

Compound	$\nu(\text{OH})/(\text{H}_2\text{O})$	$\nu(\text{C}=\text{N})$	$\nu(\text{C}-\text{O})$	$\nu(\text{C}-\text{OMe})$
1	3434	1642	1309	1231
2	3449	1639	1319	1230
3	3391	1630	1321	1230
4	3501(Assy), 3419 (sym)	1641	1313	1229

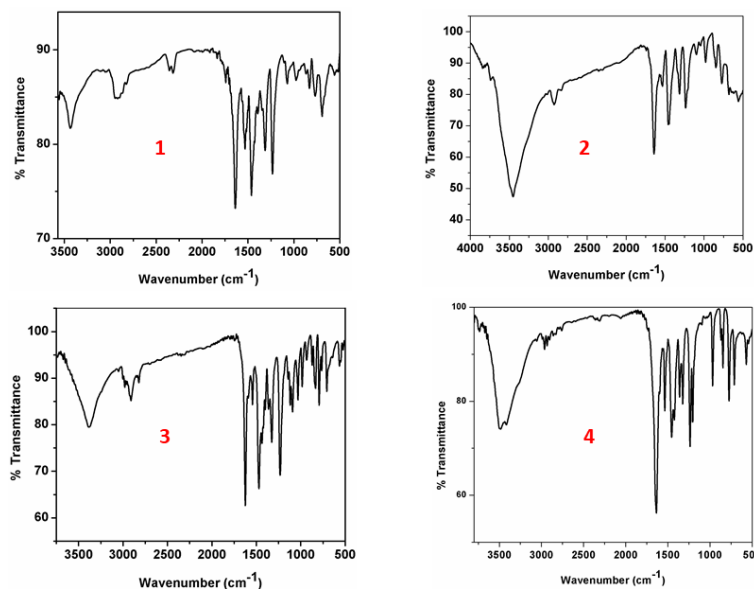


Fig. S1 IR spectra of compounds **1** to **4**.

Electronic Spectral Data

Electronic spectra of the compounds (**1** to **4**) were recorded in DMF solution at room temperature. In order to obtain the transitions other than *dd*, the spectrum was recorded in 10^{-5} M concentration whereas the *dd* bands were obtained only at higher concentration ie. 10^{-3} M concentration in the same solvent.

The peak around 400 nm in all the four compounds represents the intraligand charge transfer transition that may originate from the donor atoms such as oxygen and nitrogen to the central metal atom. The peak observed just below 300 nm which can be assigned as $\pi \rightarrow \pi^*/n \rightarrow \pi^*$ transition (Fig. S2 and Table S2). The *dd* band could be observed as a broad peak above 500 nm (Fig. S3). In the case of Cu(II) compounds the *dd* bands were originated by the hole transition from the high energy *d* orbital to the lower lying ones. In the case of compounds **1**, **3** and **4**, the *dd* band originated by the hole transition from $d_{x^2-y^2}$ to the lower energy orbitals. These transitions can be assigned as ${}^2B_{1g} \rightarrow {}^2B_{2g}$ ($d_{x^2-y^2} \rightarrow d_{xy}$), ${}^2B_{1g} \rightarrow {}^2A_{1g}$ ($d_{x^2-y^2} \rightarrow d_z^2$) and ${}^2B_{1g} \rightarrow {}^2E_g$ ($d_{x^2-y^2} \rightarrow d_{xz}, d_{yz}$) in compounds since they have square planar or near square pyramidal geometry. Since the four low-lying orbitals have little energy difference between them, the individual transfer between these orbitals and the upper *d* level cannot be resolved into three bands and hence a single absorption band is observed.^{1,2} The compound **1** has a distorted square-pyramidal geometry hence the second most ene rgised state is d_z^2 . The compound **2** adopts a trigonal bipyramidal geometry (TBP) so the hole transition are originated from of the d_z^2 orbital instead of $d_{x^2-y^2}$ to the lower energy degenerate $d_{xy}, d_{x^2-y^2}$ and d_{xz}, d_{yz} orbitals ie. $d_z^2 \rightarrow d_{xy}, d_{x^2-y^2}$ and $d_z^2 \rightarrow d_{xz}, d_{yz}$.

Table S2 Electronic spectra of compounds **1** to **4** in nm

Compound	Intraligand transitions(10^{-5} M)	<i>dd</i> band
	ϵ in brackets	(10^{-3} M)
1	270 (62,700), 370 (6,700)	594 (63)
2	283 (23,000), 377 (4,700)	597 (250)
3	284 (23,000), 378 (8,000)	580 (221)
4	283 (32,000), 376 (11,000)	614 (253)

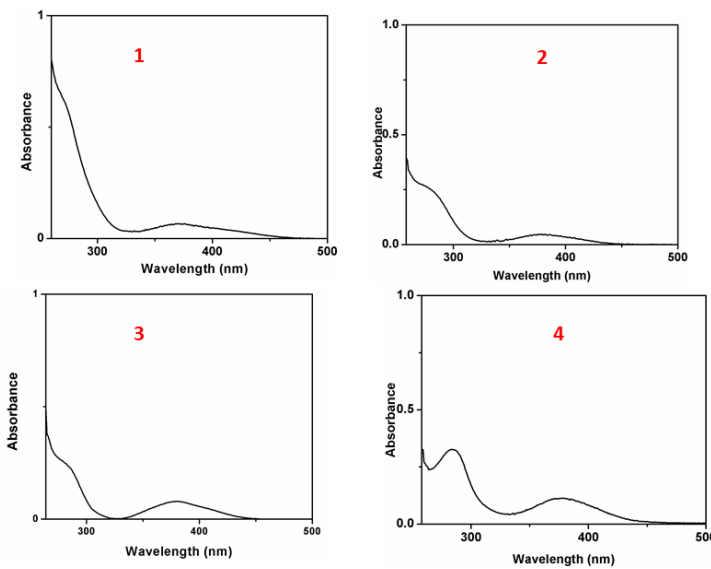


Fig. S2 Intraligand transitions of compounds **1** to **4**.

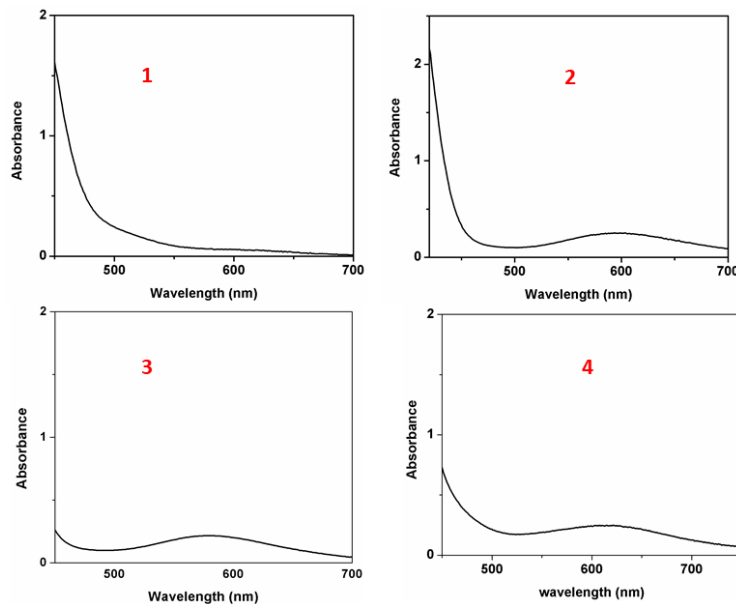


Fig. S3 *dd* band of compounds **1** to **4**.

Table S3 Crystal data and structural refinement parameter of compound **1**, **2** and **4**

Compound	1	2	4
Empirical formula	C ₂₁ H ₂₄ Br ₂ N ₂ O ₅ Cu	C ₁₈ H ₁₈ Br ₂ CuN ₂ O ₅	C ₂₁ H ₂₇ CuN ₂ O ₆
CCDC	1915472	2142350	2142351
Formula weight	607.78	565.70	467
Color	Dark Green	Dark Green	Dark Green
Crystal system	Monoclinic	Orthorhombic	Monoclinic
Space group	P2 ₁ /c	Pnma	C2/c

Cell parameters			
a (Å)	12.80 (10)	8.740 (8)	23.61 (19)
b (Å)	12.57 (9)	28.03 (5)	9.489 (6)
c (Å)	14.21(10)	8.00(8)	20.94(18)
α (°)	90	90	90
β (°)	99.73	90	112.9
γ (°)	90	90	90
Volume V (Å³)	2256.1(3)	1960(4)	4322.4(6)
Z	4	4	4
Calculated density (ρ) (Mg m⁻³)	1.789	1.917(4)	1.435
Absorption coefficient, μ (mm⁻¹)	4.546	5.223	1.050
F(000)	1212	1116	1952
Crystal size mm³	0.50 x 0.45 x 0.40	0.52 x 0.46 x 0.48	0.300 x 0.200 x 0.200
θ (°) range for data collection	2.55 to 28.41	2.647 to 28.139	2.715 to 28.49
Limiting indices	-17 ≤ h ≤ 17, -16 ≤ k ≤ 16, -18 ≤ l ≤ 18	-11 ≤ h ≤ 11, -33 ≤ k ≤ 18, -10 ≤ l ≤ 8	-31 ≤ h ≤ 31, -12 ≤ k ≤ 10, -28 ≤ l ≤ 27
Reflections collected	7445	7445	17280
Unique Reflections (R_{int})	5598 (0.0355)	7665 (0.0797)	5471 (0.0292)
Absorption correction	Semi-empirical from equivalents	Semi-empirical from equivalents	Semi-empirical from equivalents
Maximum and minimum transmission	0.708 and 0.532	0.708 and 0.532	0.825 and 0.792
Refinement method	Full-matrixleast- squares on F^2	Full-matrixleast- squares on F^2	Full-matrixleast- squares on F^2
Data / restraints / parameters	4211 / 0 / 288	2007 / 14 / 143	5471 / 0 / 284
Goodness-of-fit on F^2	1.072	1.026	1.031
Final R indices [$I > 2\sigma$ (I)]	$R_1 = 0.0376$ $wR_2 = 0.1061$	$R_1 = 0.0531$ $wR_2 = 0.0996$	$R_1 = 0.0346$ $wR_2 = 0.0925$
R indices (all data)	$R_1 = 0.0626$ $wR_2 = 0.1245$	$R_1 = 0.1305$ $wR_2 = 0.1199$	$R_1 = 0.0529$ $wR_2 = 0.1028$
Largest difference peak and hole (e Å⁻³)	0.7820 and -0.656	0.556 and -0.721	0.302 and -0.390

$$R_1 = \frac{\sum |F_o| - |F_c|}{\sum |F_o|} \quad wR_2 = \left[\frac{\sum w(F_o^2 - F_c^2)^2}{\sum w(F_o^2)^2} \right]^{1/2}$$

Table S4 Selected bond lengths and angles of **1** obtained through X-ray and DFT studies

Bond lengths	Experimental	B3LYP/def2- TZVP	Bond angles	Experimental	B3LYP/def2- TZVP
-----------------	--------------	---------------------	-------------	--------------	---------------------

Cu(1)–O(3)	1.93(2)	1.86	O(3)–Cu(1)–O(1)	90.6(9)	85.4
Cu(1)–O(1)	1.94(2)	1.86	O(3)–Cu(1)–N(2)	177(10)	94.3
Cu(1)–N(2)	1.96(3)	1.87	O(1)–Cu(1)–n(2)	91.5(10)	179
Cu(1)–N(1)	1.97(3)	1.87	O(3)–Cu(1)–N(1)	90.4(10)	179
Cu(1)–O(1W)	2.34(3)	1.28	O(1)–Cu(1)–N(1)	156.1(11)	94.3
			N(2)–Cu(1)–N(1)	87.9(11)	85.7
			O(3)–Cu(1)–O(1W)	92.9(10)	128.
			O(1)–Cu(1)–O(1W)	97.4(10)	128

Table S5 Hydrogen bonding and other supramolecular interactions present in **1**

Hydrogen bonding interactions				
D–H…A	D–H (Å)	H…A (Å)	D…A (Å)	∠D–H…A (°)
O(1W)–H(1W)…O(1)	0.84	2.19	2.85	137
O(1W)–H(1W)…O(2)	0.84	2.31	3.05	147
O(1W)–H(1W)…O(3)	0.85	2.17	2.92	149
O(1W)–H(1W)…O(4)	0.85	2.38	3.07	139
Cg … Cg interactions				
Cg … Cg		C–H … π	Metal … π	
Cg(4) … Cg(5) = 3.58 (Å)		–	–	
Cg(4) = C(1) – C(2) – C(3) – C(4) – C(5) – C(6)				
Cg(5) = C(14) – C(15) – C(16) – C(17) – C(18) – C(19)				

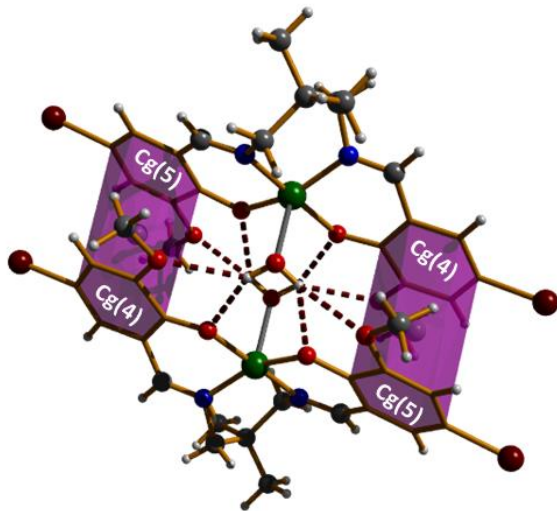


Fig. S4 $\pi \cdots \pi$ interactions in the supramolecular dimer of **1** (For clarity only water hydrogens are shown).

Table S6 Selected bond lengths and bond angles of compound **2**

	Bond lengths (\AA)		Bond angles ($^\circ$)
Cu(1)–N(1)	1.950(5)	O(2)–Cu(1)–N(1)	166.40(2)
Cu(1)–N(2)	1.950(5)	O(2)–Cu(1)–N(2)	91.85(6)
Cu(1)–O(1)	1.931(4)	O(1)–Cu(1)–N(1)	91.85(19)
Cu(1)–O(2)	1.931(4)	O(1)–Cu(1)–N(2)	166.49(6)
O(1)–C(6)	1.306(7)	N(1)–Cu(1)–N(2)	82.50(3)
O(2)–C(16)	1.304(2)	O(1)–Cu(1)–O(2)	90.20(2)
N(1)–C(8)	1.479(2)	C(7)–O(1)–Cu(1)	127.30(3)
N(2)–C(9)	1.527(10)	C(8)–N(1)–Cu(1)	127.14 (4)

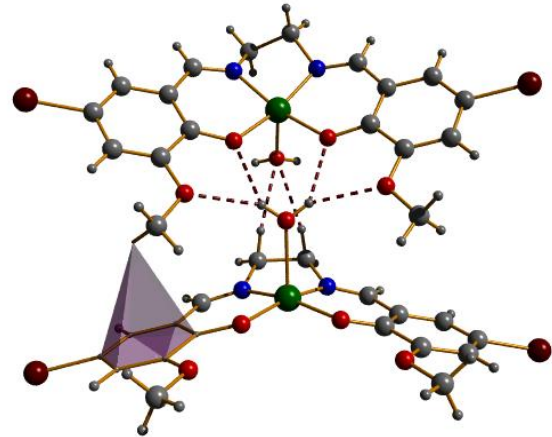


Fig. S5 Formation of a dimer through different interactions in **2**.

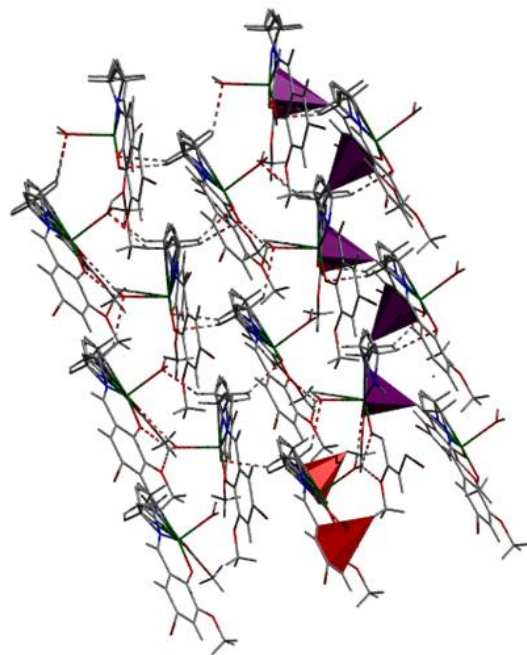


Fig. S6 Formation of a 1-D sheet including the helical propagation via two different $\text{C}-\text{H}\cdots\pi$ interactions in **2**.

Table S7 Hydrogen bonding and other supramolecular interactions present in 2

Hydrogen bonding interactions				
D–H···A	D–H (Å)	H···A (Å)	D···A (Å)	∠D–H···A (°)
O(1W)–H(1W)···O(1)	0.82	2.28	2.90	140
O(1W)–H(1W)···O(2)	0.82	2.23	2.97	150
O(1W)–H(1W)···O(3)	0.97	2.57	3.37	140
O(1W)–H(1W)···O(4)	0.97	2.56	3.36	136
C(9)–H(9A)···O(5)	0.97	2.57	3.37	140
C(10)–H(10D)···O(1)	0.97	2.56	3.36	136
CH ··· π interactions		C–H ··· π	Metal ··· π	
Cg(6) ··· H(1C) – C(1)	2.99 (Å)	–	–	
Cg(6) ··· H(8) – C(8)	2.98 (Å)	–	–	
Cg(4) ··· H(10A) – C(10)	2.93 (Å)	–	–	
Cg(6) = C(2) – C(3) – C(4) – C(5) – C(6) – C(7)	–	–	–	
Cg(4) = Cu(1) – O(1) – C(7) – C(6) – C(8) – N(1)	–	–	–	

Table S8 Selected bond lengths and bond angles of compound 4

Bond lengths (Å)		Bond angles (°)	
Cu(1)–N(1)	1.946(13)	O(2)–Cu((1)–N(1)	94.15(7)
Cu(1)–N(2)	1.936(16)	O(2)–Cu((1)–N(2)	156.75(7)
Cu((1)–O(2)	1.885(13)	O(3)–Cu((1)–N(2)	93.57(6)
Cu((1)–O(3)	1.900 (14)	O(3)–Cu((1)–N(1)	155.13(6)
O(1)–C(20)	1.420(3)	N(1)–Cu((1)–N(2)	92.18(7)
O(4)–C(21)	1.413 (3)	O(1)–Cu((1)–O(2)	90.02(6)
N(1)–C(7)	1.279(2)	C(1)–C(2)–C(6)	119.93(14)
N(1)–C(8)	1.460(2)	C(3)–C(4)–C(5)	120.6(2)
N(2)–C(12)	1.454(3)		
N(2)–C(13)	1.285(3)		

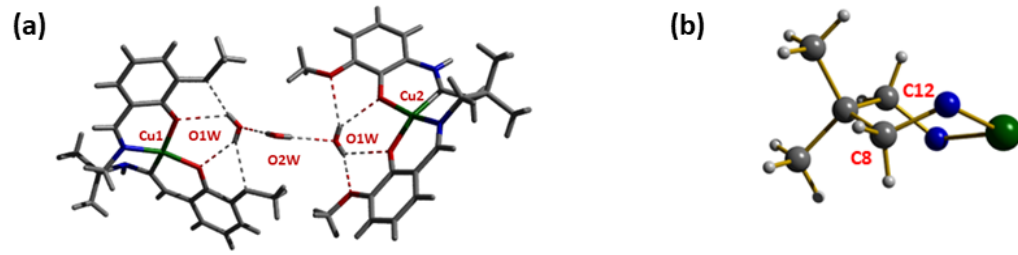


Fig. S7 (a) Formation of a dimer through hydrogen bonding interaction (b) Twist boat conformation of a metallocycle in 4.

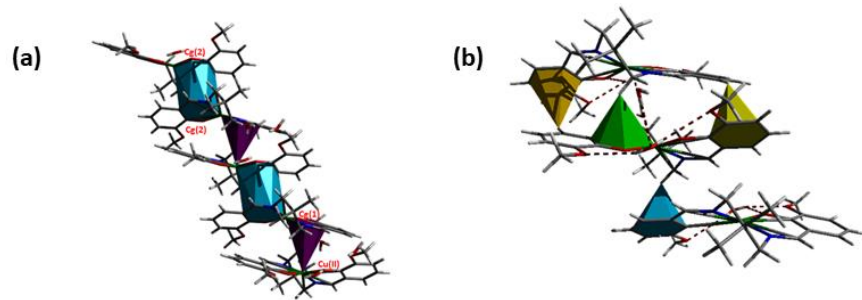
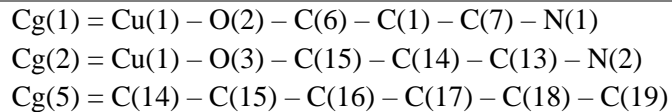


Fig. S8 (a) Stair-like architecture through $\pi \cdots \pi$ and metal $\cdots \pi$ interactions (b) Different types of C–H $\cdots \pi$ interactions in 4.

Table S9 Hydrogen bonding and other supramolecular interactions present in 4

Hydrogen bonding interactions				
D–H···A	D–H (Å)	H···A (Å)	D···A (Å)	$\angle D\text{--}H\cdots A$ (°)
O(1w)–H(1w)···O(1)	0.76	2.21	2.92	157
O(1w)–H(1w)···O(2)	0.76	2.49	3.01	128
O(1w)–H(1w)···O(3)	0.67	2.31	2.88	144
O(1w)–H(1w)···O(4)	0.67	2.42	3.09	149
O(2w)–H(2w)···O(1w)	0.68	2.24	2.92	176
Cg \cdots Cg interactions	CH \cdots π interactions		Metal \cdots π interactions	
Cg(2) \cdots Cg (2) 3.44 Å	C2–H2 \cdots Cg(5) 2.81 Å		Cu(1) \cdots Cg(1) 3.84 Å	
	C8–H8B \cdots Cg(5) 2.84 Å			



4.3.2. Characterization of Compound 3

We have made several attempts to crystallize the compound but not able to isolate single crystals. So we have characterised the compounds with other spectroscopic techniques.

Compound 3 (CuL3) : Yield (72%); FTIR/cm⁻¹ (KBr) 3391 (–OH st) 2910 (CH_{st}), 1630 (C=N), 1465 (Ar C=C), 1321 (C-O phenolic), 1230 (C-O methoxy) (Table 4.1, Fig. 4.1). Mass data: 560.89 (M+2, 100%). Anal. calc. for C₁₉H₁₈N₂Br₂CuO₄: C, 40.63 ; H, 3.23 ; N, 4.99. Found C, 40.63 ; H, 3.23 ; N, 4.99 %.

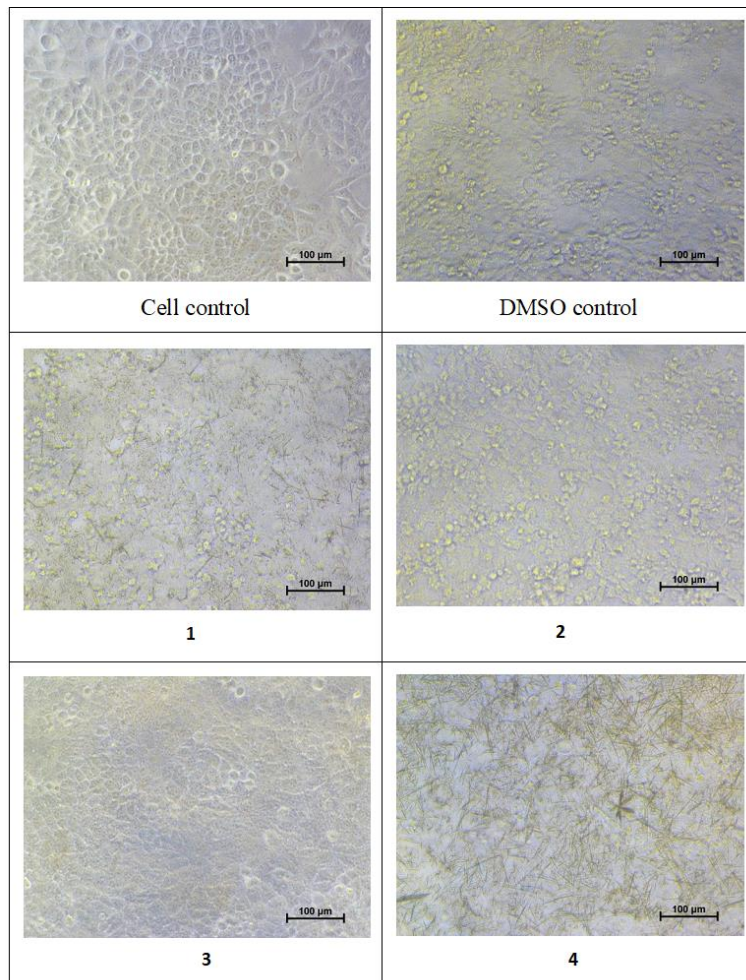


Fig S9 Inverted phase contrast microscope images of HeLa cells treated with Cu(II) compounds at 37 °C for 24 hours. Images of DMSO alone and untreated cells were presented for reference.

(Objective: 20x)

Table S10 MTT assay values of the compounds

Compound	Concentration ($\mu\text{g/L}$)
1	71.73
2	132.78
3	122.53
4	47.00
DMSO	111.49
Cell	100.0

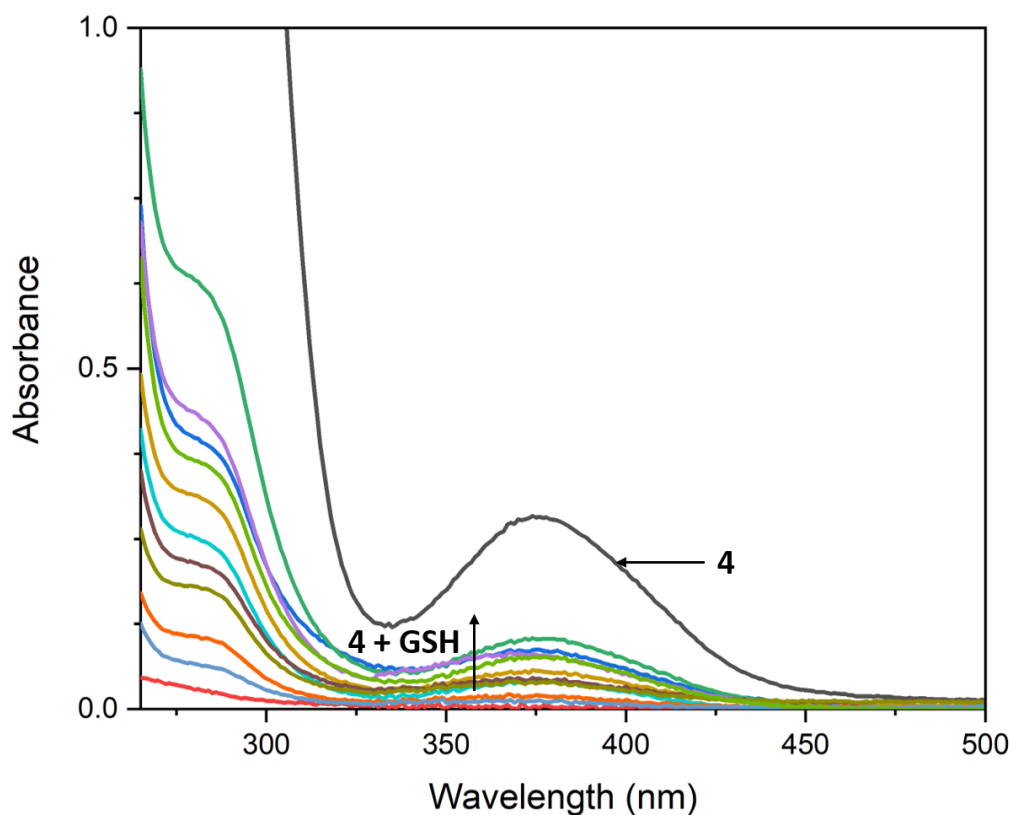


Fig. S10 UV-Vis spectra of **4** along and the incremental addition of GSH to **4**

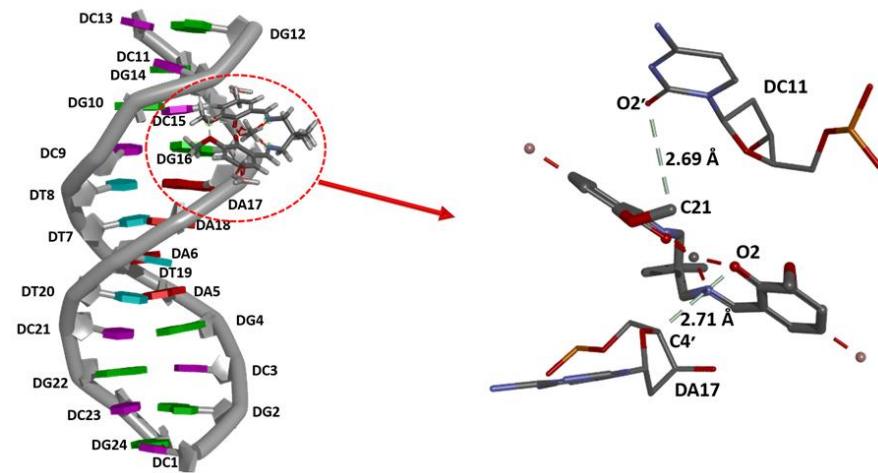


Fig. S11 Docked model of compound **1** with B-DNA showing major supramolecular interactions present.

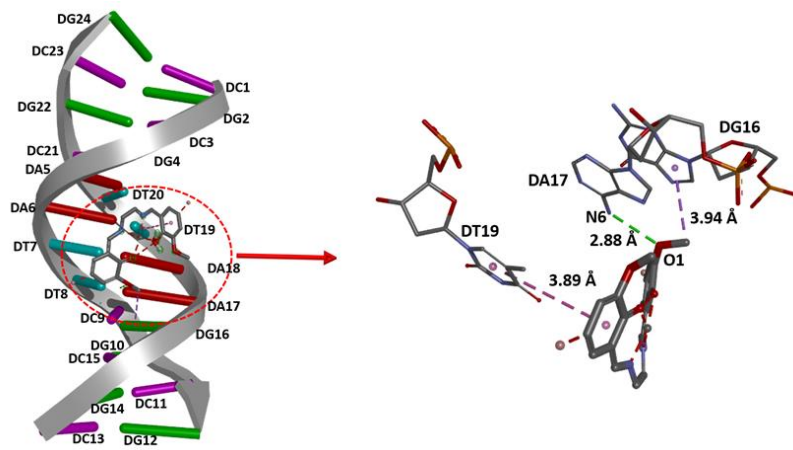


Fig. S12 Docked model of compound **2** with B-DNA showing major supramolecular interactions present.

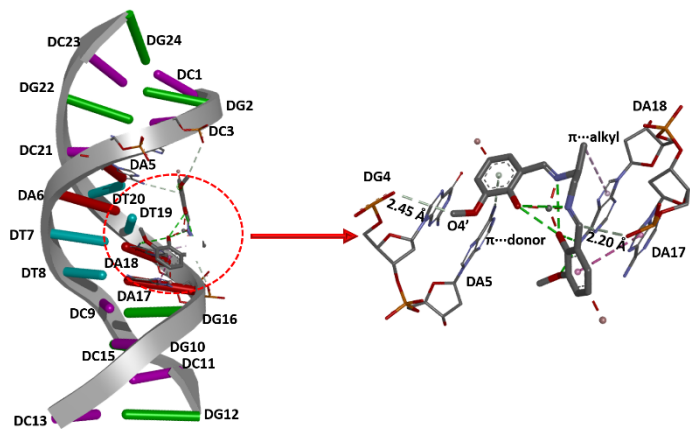


Fig. S13 Docked model of compound **3** with B-DNA showing major supramolecular interactions present.

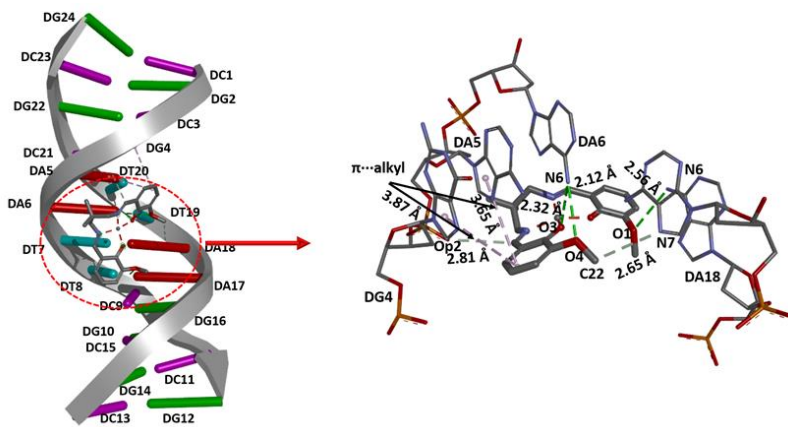


Fig. S14 Docked model of compound **4** with B-DNA showing major supramolecular interactions present.

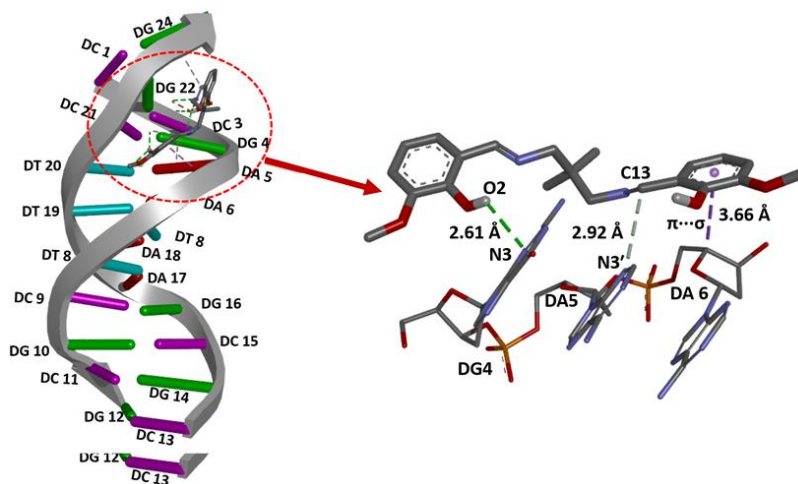


Fig. S15 Docked model of the ligand of compound **4** with B-DNA showing major supramolecular interactions present.

Table S11 Docking scores of compounds (**1** to **4**) with B-DNA and HSA

Compounds	1	2	3	4	H₂L4
B-DNA (kcal/mol)	-7.7	-7.6	-8.1	-8.2	-6.0
HSA (kcal/mol)	-7.2	-6.5	-7.5	-7.6	-6.3

Table S12 The interactions between the compounds (**1** to **4** and **H₂L4**) and B-DNA

Compound	Base	D-H...A	D...A
1	Cytosine (DC11)	C21-H21C...O2'	2.69 Å
	Adenine (DA17)	C4'-H4'...O2	2.71 Å
	Adenine (DA17)	N6-H6B...O1	2.88 Å
2	Guanine (DG16)	$\pi \cdots \sigma$	3.94 Å
	Thymine (DT19)	$\pi \cdots \pi$ interaction (T-type)	3.89 Å
	Guanine (DG4)	C20-H20A...O4'	2.45 Å
3	Adenine (DA17)	C12-H12...O4	2.20 Å
	Adenine (DA17)	$\pi \cdots \pi$ interaction (T-type)	3.40 Å
	Adenine (DA18)	$\pi \cdots$ alkyl	3.22 Å
	Adenine (DA05)	$\pi \cdots$ donor interaction	3.65 Å
	Adenine (DA06)	N6-H6B...O4	2.32 Å
	Adenine (DA18)	N6-H6A...O1	2.56 Å
	Adenine (DA18)	C22-H22A...N7	2.65 Å

	Phosphate bridging between adenine (DA5) and guanine units (DG4)	C14–H14A···Op2	2.81 Å
4	Guanine (DG4)	π ···alkyl	3.65 Å
	Adenine (DA5)	π ···alkyl	3.87 Å
H₂L4	Guanine (DG04)	O2–H2···N3	2.61 Å
	Adenine (DA05)	C13–H13···N3'	2.32 Å
	Adenine (DA06)	π ··· σ	3.66 Å

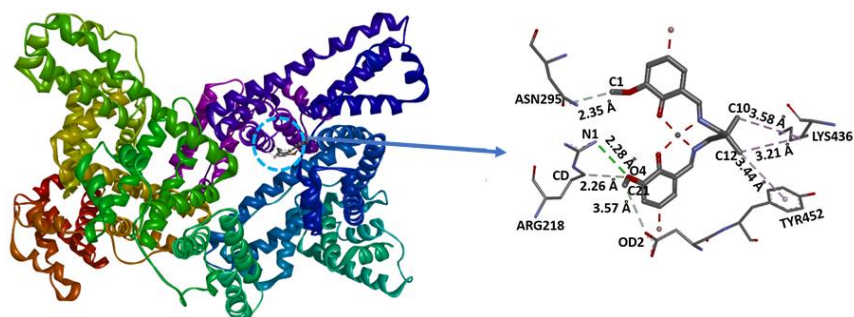


Fig. S16 Docked model of compound **1** with HSA showing major supramolecular interactions present.

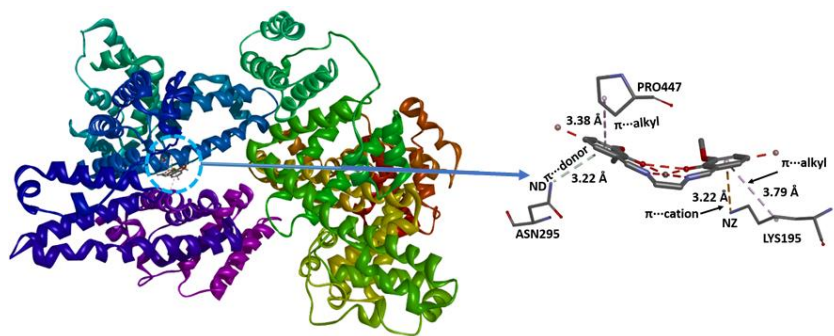


Fig. S17 Docked model of compound **2** with HSA showing major supramolecular interactions present.

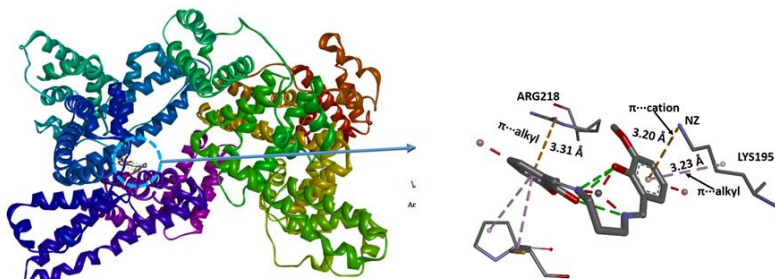


Fig. S18 Docked model of compound **3** with HSA showing major supramolecular interactions present.

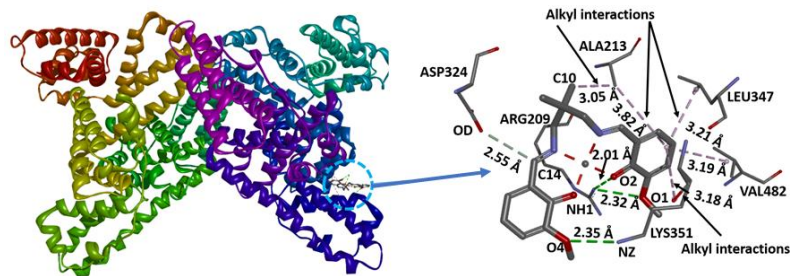


Fig. S19 Docked model of compound **4** with HSA showing major supramolecular interactions present.

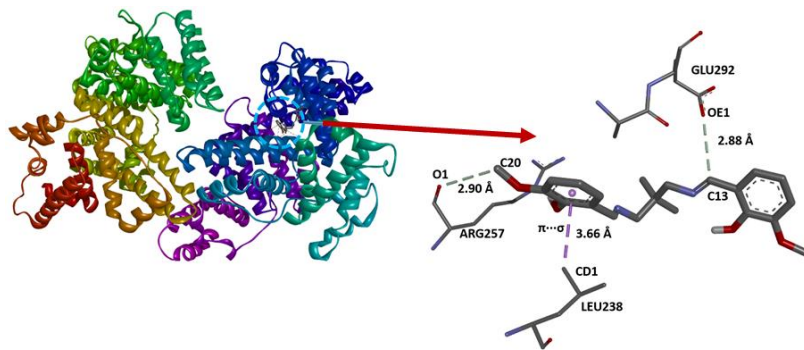


Fig. S20 Docked model of **H₂L4** with HSA showing major supramolecular interactions present.

Table S13 The interactions between the compounds (**1** to **4** and ligand of **4**) and HSA protein

Compound	Amino acid	D–H···A	D···A
1	Arginine (ARG218)	CD–H1D···O4	2.26 Å
	Arginine (ARG218)	N1–H1···O4	2.28 Å
	Asparagine (ASN295)	C1–H1A···OD1	2.35 Å
	Lysine (LYS436)	Alkyl interaction	3.21 Å
	Lysine (LYS436)	Alkyl interaction	3.58 Å
	Tyrosine (TYR452)	π···alkyl	3.44 Å
2	Asparagine (ASN295)	π···donor hydrogen interaction	3.22 Å
	Lysine (LYS195)	π···cation	3.22 Å
	Proline (PRO447)	π···alkyl interaction	3.38 Å
3			

Lysine (LYS195)	$\pi\cdots$ alkyl	3.23 Å
Arginine (ARG218)	$\pi\cdots$ alkyl	3.31 Å
Lysine (LYS195)	$\pi\cdots$ cation	3.27 Å
4		
Arginine (ARG209)	N1–H1A···O2	2.01 Å
Arginine (ARG209)	N1–H1B···O1	2.32 Å
Lysine (LYS351)	Nz–HzB···O4	2.35 Å
Aspartic acid (ASP362)	C22–H22A···N7	2.55 Å
Alanine (ALA213)	$\pi\cdots$ alkyl	3.05 Å and 3.82 Å
Leucine (LEU347)	$\pi\cdots$ alkyl	3.21 Å and 3.80 Å
Lysine (LYS351)	$\pi\cdots$ alkyl	3.18 Å
Valine (VAL482).	$\pi\cdots$ alkyl	3.19 Å
H₂L4		
Glutamic (GLU 292)	C13–H13···OE1	2.88 Å
Arginine (ARG 257)	C20–H20A···O1	2.90 Å
Lysine (LEU 238)	$\pi\cdots\sigma$	3.66 Å

References

1. A. Sreekanth and M. R. P. Kurup, *Polyhedron*, 2003, **22**, 3321-3332.
2. B. Hathaway, G. Wilkinson, R. Gillard and J. McCleverty, *Journal*, 1987.